PNAS
www.pnas.org

Supplementary Information for

Spastin is a dual function enzyme that severs microtubules and promotes their regrowth to increase the number and mass of microtubules

Yin-Wei Kuo, Olivier Trottier, Mohammed Mahamdeh, Jonathon Howard

Corresponding author: Jonathon Howard
Email: jonathon.howard@yale.edu

This PDF file includes:

Appendix
Figs. S1 to S5
References for SI reference citations

Other supplementary materials for this manuscript include the following:

Movies S1 to S3

www.pnas.org/cgi/doi/10.1073/pnas.1818824116

Appendix

We extended the previously described dynamic instability model in Dogterom & Leibler (1) to incorporate microtubule severing. As described in main text, we assumed that: (i) severing takes place at random positions on microtubules with equal probability. The severing rate is defined as k with the unit length^{-1}time^{-1}. (ii) Severing generates a new stable minus end and a new shrinking plus end that shorten with the rate v_s. For the model scheme, see Fig. 3A. The master equations are

$$\frac{\partial n_g}{\partial t}(x,t) = -v_g \frac{\partial n_g}{\partial x}(x,t) - f_{gs} n_g(x,t) + f_{sg} n_s(x,t) - kx n_g(x,t) + k\int_x^\infty n_g(y,t)dy \qquad \text{Eq. 1}$$

$$\frac{\partial n_s}{\partial t}(x,t) = v_s \frac{\partial n_s}{\partial x}(x,t) + f_{gs} n_g(x,t) - f_{sg} n_s(x,t) - kx n_s(x,t) + k\int_x^\infty \left[n_g(y,t) + 2n_s(y,t)\right]dy \qquad \text{Eq. 2}$$

where $n_g$and n_s are number of growing and shrinking microtubules with length x at time t with $x > 0$. Microtubule dynamics parameters v_g, v_s, f_{gs}, f_{sg} are growth rate, shrinkage rate, catastrophe frequency and rescue frequency respectively. The master equations are identical to equation 8 and 9 in Tindemans & Mulder (2), where they solved for microtubule length distribution in the presence of severing under spontaneous nucleation conditions. Summing the two lines in Eq. 2 gives an equation for the net change in filament length; this is identical to equation 12 in Ermentrout & Eldelstein-Keshet (3).

Summing Eq.1 and 2 and integrating over length, we get the rate of change of the total number of microtubules, assuming that all microtubules have finite length:

$$\frac{\partial N}{\partial t}(t) = v_g n_g(0^+,t) - v_s n_s(0^+,t) + kM(t) \qquad \text{Eq. 3}$$

where $N(t)$ and $M(t)$ are the total number of microtubules and total microtubule polymer mass at time t. The flux of total polymer mass can be obtained by multiplying both Eq.1 and 2 by x, summing and integrating over length:

$$\frac{\partial M}{\partial t}(t) = \int_0^\infty x \frac{\partial n}{\partial t}(x,t)dx = v_g N_g(t) - v_s N_s(t) \qquad \text{Eq. 4}$$

N_g and N_s are the total numbers of growing and shrinking microtubules.

Differentiating Eq.4 with respect to time and combining with Eq.1 and 2 we get:

$$\begin{aligned}\ddot{M} &= v_g \frac{\partial N_g}{\partial t} - v_s \frac{\partial N_s}{\partial t} \\ &= \left[v_g^2 n_g(0^+,t) + v_s^2 n_s(0^+,t)\right] - \left(f_{gs} + f_{sg}\right)\dot{M} - \left(f_{gs} v_s - f_{sg} v_g\right)N - k v_s M. \qquad \text{Eq. 5}\end{aligned}$$

We focus on the condition when microtubule length distribution reaches steady state and solve Eq.3 as:

$$N(t) = A\exp\left(\left[v_g p_g(0^+,t) - v_s p_s(0^+,t) + k\bar{x}\right]t\right) \qquad \text{Eq. 6}$$

where $p_g(x,t)$ and $p_s(x,t)$ are probability densities of growing and shrinking microtubules with length x at time t, $\bar{x}$ is the mean microtubule length and A is a positive constant.

This shows that the number of microtubules will increase or decrease exponentially when the length distribution reaches a steady state.

Now we consider two possible boundary conditions. When there is a stable seed at the minus end, the gain of new growing MTs of zero length (i.e. seeds) matches the loss of old microtubules disappearing and we can write the boundary condition as:

$$v_g n_g(0^+,t) = v_s n_s(0^+,t) \;\text{ or }\; v_g p_g(0^+,t) = v_s p_s(0^+,t)$$

In this situation, $N(t) = A\exp(k\bar{x}t)$ and thus microtubule number and polymer mass increase exponentially with the characteristic time $1/k\bar{x}$.

The other condition is that there is no stable seed and a microtubule will disappear when it shrinks all the way back to the minus end. In this case, the boundary condition is:

$$n_{\mathrm{g}}(0^+, t) = p_{\mathrm{g}}(0^+, t) = 0$$

Eq.6 can be rewritten as: $N(t) = A\exp([k\bar{x} - v_s p_s(0^+, t)]\,t)$. When $k\bar{x} - v_{\mathrm{s}}p_{\mathrm{s}}(0^+, t) > 0$, both the number of microtubules and the polymer mass increase exponentially. Substituting this solution of $N(t)$ into Eq.5 and divide both sides by $N(t)$ we get a characteristic equation:

$$\bar{x}(k\bar{x} - v_{\mathrm{s}}p_{\mathrm{s}}(0^+))^2 + \bar{x}\big(f_{\mathrm{gs}} + f_{\mathrm{sg}}\big)\big(k\bar{x} - v_{\mathrm{s}}p_{\mathrm{s}}(0^+)\big) + v_{\mathrm{s}}\big(k\bar{x} - v_{\mathrm{s}}p_{\mathrm{s}}(0^+)\big) - \big(f_{\mathrm{sg}}v_{\mathrm{g}} - f_{\mathrm{gs}}v_{\mathrm{s}}\big) = 0 \quad \mathrm{Eq.}\,7$$

This equation will only have a positive root for $k\bar{x} - v_s p_s(0^+)$ when the constant term $f_{\mathrm{sg}}v_{\mathrm{g}} - f_{\mathrm{gs}}v_{\mathrm{s}} > 0$, corresponding to the unbounded growth condition $v_{\mathrm{g}}/f_{\mathrm{sg}} - v_{\mathrm{s}}/f_{\mathrm{gs}} > 0$ and the average flux $(v_{\mathrm{g}}f_{\mathrm{sg}} - v_{\mathrm{s}}f_{\mathrm{gs}})/(f_{\mathrm{sg}} + f_{\mathrm{gs}}) > 0$ in Dogterom & Leibler's dynamic instability model (1). Thus, from our mathematical model, we conclude that to increase total microtubule number and polymer mass by severing, the microtubule dynamics parameters have to be in the regime of unbounded growth.

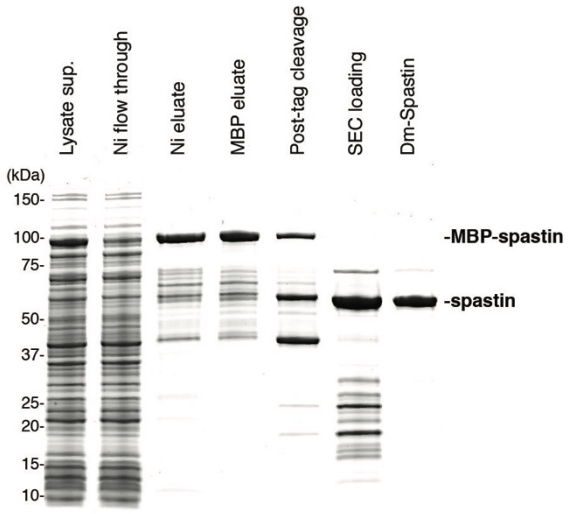

Fig. S1. SDS-PAGE gel of Drosophila melanogaster spastin purification. His-MBP-spastin appears as a 102 kD band prior to TEV protease tag cleavage. After cleaving off the His-MBP tag, Drosophila spastin appears as a 62 kD band. Final product purity > 97%, estimating from the SDS-PAGE band intensity.

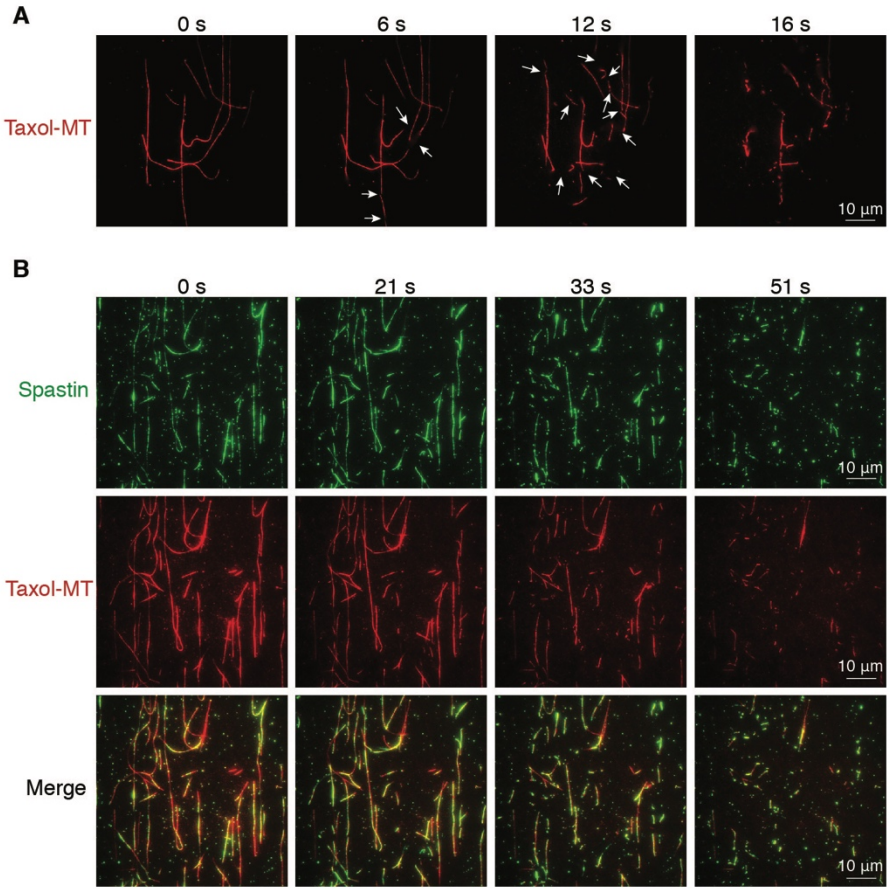

Fig. S2. *In vitro* microtubule severing assay. (A) Purified Drosophila spastin (20 nM, unlabeled) severed taxol-stabilized microtubules (red). TAMRA-labeled taxol-stabilized microtubules were visualized by total internal reflection fluorescence (TIRF) microscopy. White arrows showed the breakages of microtubules produced by severing. (B) Fluorescently labeled spastin (35 nM) severed taxol-MTs imaged by dual-color TIRF microscopy. Green: Dylight488-spastin; red: taxol-MT (TAMRA).

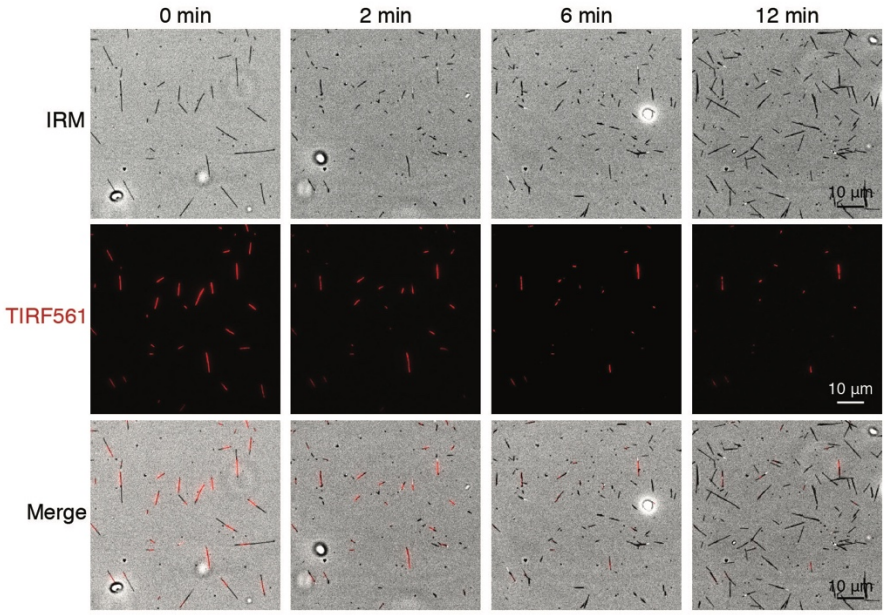

Figure S3. Dynamic microtubule severing assay imaged by IRM and TIRF microscopy. GMPCPP-MT seeds were labeled with TAMRA and were visualized with TIRF microscopy. The dynamic microtubules with unlabeled tubulin were imaged by IRM. Both dynamic microtubules and GMPCPP-MT were severed by spastin. The majority of the newly generated microtubules showed no red fluorescence signal in the TIRF channel, indicating that these microtubules were not directly polymerized from severed GMPCPP-MT fragments.

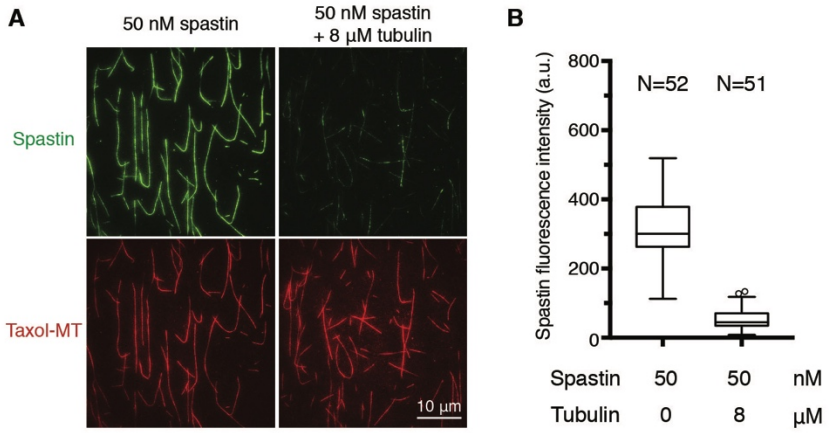

Figure S4 Free tubulin inhibits microtubule binding affinity of spastin. (A) DyLight488-labeled spastin molecules decorate TAMRA-labeled taxol-stabilized microtubules in the absence of adenosine nucleotide, imaged by TIRF microscopy. Left: 50 nM spastin only; right: 50 nM spastin with 8 μM unlabeled bovine tubulin (no GTP). (B) Average spastin fluorescent intensity per microtubule in the presence or absence of free tubulin. The microtubule binding affinity of spastin is greatly reduced (~7 times) in the presence of free tubulin. The midline of each box shows the median value, the upper and bottom show the 75th and 25th percentiles, and the whiskers are 1.5 interquartile range from the 75th and 25th percentiles. Outliers (outside the whisker range) are represented with empty circles. Sample size *N* indicates the number of microtubules analyzed in each condition

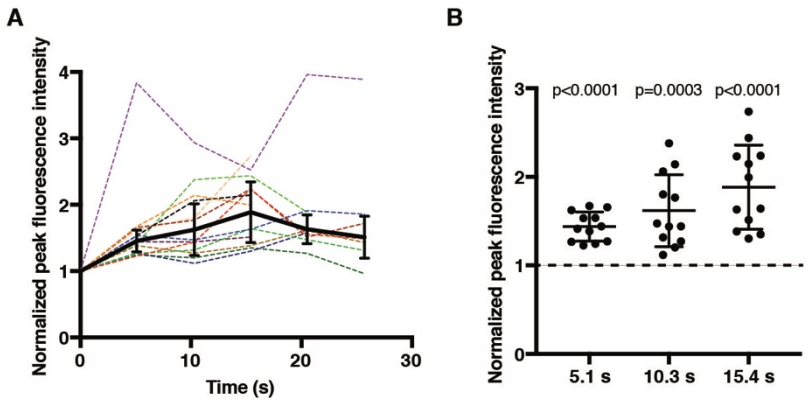

Figure S5 Time course intensity change of DyLight488-spastin on shrinking microtubule tips in the presence of ATP. (A) Normalized time course intensity change of DyLight488-spastin in TIRF from 13 microtubules. Peak intensity of spastin signal on microtubule ends was measured and normalized by the intensity of the first frame of each trace where the shrinkage starts. Color dashed lines: traces from 13 microtubules; black line: average trace excluding the outlier (violet dashed line). Error bar: S.D. The traces show that the intensity of spastin typically increase over the first 10-15 seconds. (B) Normalized peak intensity of the first three time points after shrinkage takes place (outlier excluded). The accumulation of spastin is observed consistently for all three time points. One sample *t*-test showed that in all three time points, the normalized intensity is significantly larger than 1 ($p<0.0005$ for all three cases).

Movie S1. Asymmetric behaviors of two microtubule ends generated after severing. See Figure 3A, B.

Movie S2. Accumulation and tracking of fluorescent spastin on shrinking microtubule plus end in the presence of AMP-PNP. Upper: IRM channel; lower: TIRF channel (488 nm). See Figure 5A, B.

Movie S3. Accumulation of fluorescent spastin on shrinking microtubule plus end generated by severing in the presence of ATP. Upper: IRM channel; lower: TIRF channel (488 nm). See Figure 5C.

References

1. Dogterom M, Leibler S (1993) Physical aspects of the growth and regulation of microtubule structures. *Phys Rev Lett* 70(9):1347–1350.

2. Tindemans SH, Mulder BM (2010) Microtubule length distributions in the presence of protein-induced severing. *Phys Rev E* 81(3):2821–8.

3. Ermentrout GB, Edelstein-Keshet L (1998) Models for the length distributions of actin filaments: II. Polymerization and fragmentation by gelsolin acting together. *Bull Math Biol* 60(3):477–503.